Appl. Phys. B 88, 57–60 (2007)
DOI: 10.1007/s00340-007-2675-x

Applied Physics B
Lasers and Optics

H. WANG[1,2]
C. TU[1,✉]
Z. YOU[1]
F. YANG[1,2]
Y. WEI[1,2]
Y. WANG[1]
J. LI[1]
Z. ZHU[1]
G. JIA[1,2]
X. LU[1,2]

Conversion of infrared radiation into visible emission in $NaGd(WO_4)_2$:Yb^{3+}, Ho^{3+} crystals

[1] Fujian Institute of Research on the Structure of Matter, State Key Laboratory of Structural Chemistry, Chinese Academy of Sciences, Fuzhou, Fujian 350002, P.R. China
[2] Graduate School of Chinese Academy of Sciences, Beijing 100039, P.R. China

Received: 23 November 2006/Final version: 16 April 2007

ABSTRACT $NaGd(WO_4)_2$:Yb^{3+}, Ho^{3+} single crystals have been grown by the Czochralski technique along the (0 0 1) orientation. Conversion of the infrared (IR) radiation at 980 nm into the visible emission in $NaGd(WO_4)_2$ crystals containing several different concentrations of Yb^{3+} and Ho^{3+} has been investigated. The $NaGd(WO_4)_2$: 8 at. % Yb^{3+}, 4 at. % Ho^{3+} system exhibits intense red upconverted emission originating from the $^5F_5$

level. The upconversion mechanism in a Ho^{3+}-Yb^{3+} system under near infrared excitation is discussed. It is concluded that the green emission is excited by energy transfers from Yb^{3+} to Ho^{3+}, whereas excited state absorption is involved in the excitation of red emission. The emission cross-section of the $^5F_5 \rightarrow {}^5I_8$ transition at about 660 nm was estimated by using the Füchtbauer–Ladengurg formula.

PACS 78.55.Hx; 78.20.-e

1 Introduction

The process of conversion of infrared (IR) radiation into visible radiation is of great interest, due to the potential applications in upconversion lasers [1, 2], which produce radiation at wavelengths shorter than that of a pump light. Investigations of upconversion phenomena motivated us to search for new light sources emitting in the visible. Keeping with this motivation particular attention has been paid to crystals and glasses co-doped with ytterbium ions which exhibit strong and broad absorption bands matching the emission wavelength of powerful commercial laser diodes. The lack of pump bands at emission wavelengths of available laser diodes is a disadvantage of the $NaGd(WO_4)_2$:Ho^{3+} system, therefore co-doping with ytterbium is expected to provide an efficient excitation channel. Yb^{3+}, Ho^{3+} upconversion energy transfer is relatively simple compared to upconversion involving other rare-earth ions. The first Yb^{3+} sensitized Ho^{3+} green upconversion laser has been realized at 77 K in a BaY_2F_8 crystal [3]. Numerous published papers were devoted to upconversion phenomena and upconverted laser emission in crystals and glasses doped with Yb^{3+} and Ho^{3+} [4–6].

The $NaGd(WO_4)_2$ (NGW) single crystal belongs to the scheelite ($CaWO_4$) structure with the space group of $I4_1/a$. It is a uniaxial crystal. The cell parameters are as follows: $a = b = 5.243$ Å, $c = 11.384$ Å [7], $\alpha = \beta = \gamma = 90°$, $Z = 4$, $d = 7.2\ g/cm^3$ [8]. The crystal is structurally disordered due to the random distribution of the Gd^{3+} and Na^+ cations. Rare-earth activators entering the NGW lattice, substitute possible positions: Na^+, Gd^{3+} or interstitial positions, all having identical S_4 local symmetry [9].

Na-based double tungstates have less destructive phase transitions than those observed in K-based double tungstates. Due to this reason the crystal growth of $NaRE(WO_4)_2$ (RE is the rare-earth) compounds by the Czochralski (CZ) method, which allows to obtain crystals of large sizes at rather high growth-rates, have attracted attention in the last few years in RE-doped systems [10] and [11].

In this work, a detailed characterization of the upconversion luminescence properties of NGW:Yb^{3+}, Ho^{3+} crystals containing several different concentrations of dopants is described. The mechanism involved in the excitation process and the assessment of laser potential associated with upconverted red emission are presented.

2 Experimental

Because of its congruent melting, Yb^{3+}, Ho^{3+}-doped NGW crystal can be grown by the Czochralski technique. The growth procedure is similar to that of Tm^{3+}: NGW crystal described in our previous publication [12]. Single crystals of NGW, containing 4 at. % of Ho^{3+}, 4 at. % of Ho^{3+} and 8 at. % of Yb^{3+}, 1 at. % of Ho^{3+} and 8 at. % of Yb^{3+}, have been investigated. The samples used for spectroscopic measurements were optically polished to flat and parallel faces. The thickness of the samples was measured to be 0.26 cm. Room temperature polarized absorption spectra of the crystals were recorded by a Perkin-Elmer UV-VIS-NIR Spectrometer (Lambda-900). The polarized emission spectra of the crystals were recorded at room temperature by an Edinburgh Instruments FLS920 spectrophotometer. The emission spectra (Fig. 1) were performed using a continuous wave xenon arc lamp as a pump source centered at 488 nm. The polarized upconverted emission spectra (Figs. 2 and 3) were performed using a pulsed semiconductor laser diode as a pump source at 980 nm. The composition of the diode is $In_{1-x}Ga_xAs$ with

---

✉ Fax: +86-591-83714946, E-mail: tcy@fjirsm.ac.cn

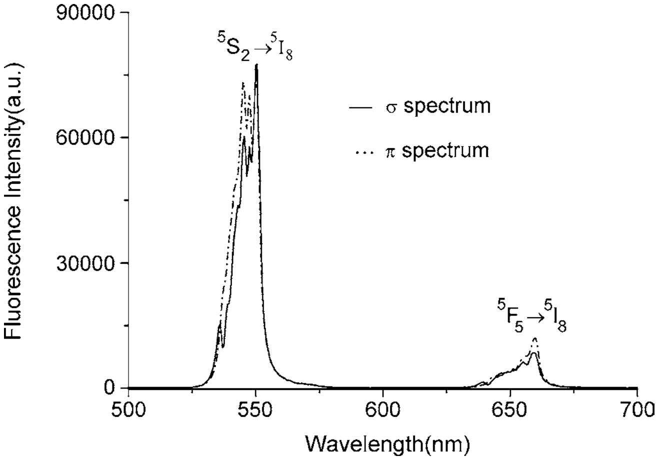

FIGURE 1 Room temperature emission spectra of the NGW: 8 at. % Yb^{3+}, 4 at. % Ho^{3+} crystal, excited by 488 nm pumping light

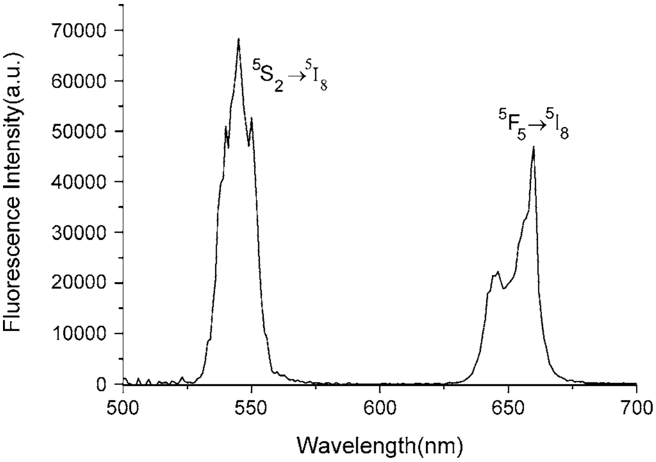

FIGURE 3 Room temperature emission spectrum of the NGW: 8 at. % Yb^{3+}, 1 at. % Ho^{3+} crystal, excited by 980 nm pumping light

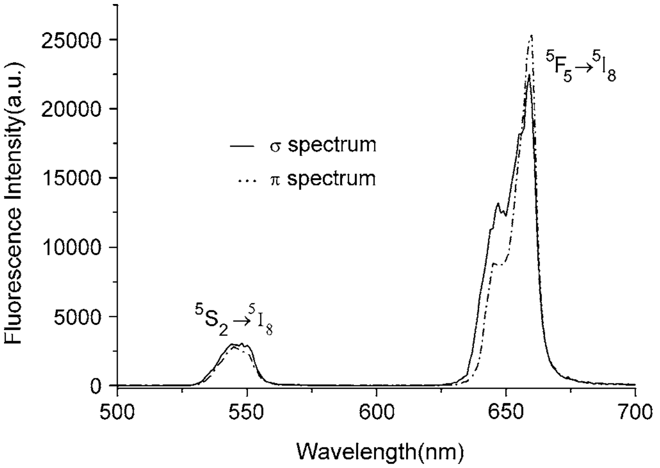

FIGURE 2 Room temperature emission spectra of the NGW: 8 at. % Yb^{3+}, 4 at. % Ho^{3+} crystal, excited by 980 nm pumping light

the linewidth of 10 nm. The highest peak power for the laser diode is 251 mW and the average power is 6 mW. Film plating is used to make the center frequency maintained at the desired wavelengths. To define the polarization of the irradiation, we used the Glan–Thompson prism to collimate the beam. The fluorescence emission was analyzed with a monochromator Acton Pro 500i and a photomultiplier tube from Hamamatsu. The resolution of both the absorption and fluorescence spectra is 1.0 nm.

3 Results and discussion

3.1 *Spectroscopic analysis*

Figure 1 shows the polarized emission spectra of the NGW crystal containing 8 at. % of Yb^{3+} and 4 at. % of Ho^{3+}, excited by 488 nm pumping light at room temperature. Two emission bands were observed, and correspond to $4f$–$4f$ transitions according to the energy diagram of the Ho^{3+} ion [13]. The green band centered at 540 nm is assigned to the $^5S_2 \rightarrow {}^5I_8$ transition and the red band centered at 660 nm is assigned to the $^5F_5 \rightarrow {}^5I_8$ transition. The ratio of integrated intensities of the green to red emission is roughly 10 : 1. Figure 2 shows the room temperature upconversion emission spectra of the NGW crystal containing 8 at. % of Yb^{3+} and 4 at. % of Ho^{3+}, excited by 980 nm pumping light. With this excitation the ratio of the intensities of the green to red emission is 1 : 10 and a bright red emission is seen with the naked eye at an excitation power as low as several milliwatts. The most remarkable feature of the red emission band is the intensity distribution in the spectra: two intense lines are centered at 647 and 660 nm. They are related to $^5F_5 \rightarrow {}^5I_8$ transitions ending at the highest crystal-field components of the $^5I_8$ terminal level. Such distribution of emission band intensity is favorable for laser performance. Moreover, it is important when the ground multiplet is the terminal level of laser transition [14]. It implies that the NGW: 8 at. % Yb^{3+}, 4 at. % Ho^{3+} crystal may be a good candidate as a medium for solid-state red lasers.

We also obtained the emission spectrum of the NGW crystal containing 8 at. % of Yb^{3+} and 1 at. % of Ho^{3+} excited by 980 nm pumping light. However, the sample containing 8 at. % of Yb^{3+} and 1 at. % of Ho^{3+} shows much stronger green emission. The ratio of integrated intensities of the green to red emission is roughly 3 : 2. The room temperature upconversion emission spectrum is presented in Fig. 3.

3.2 *Upconversion mechanism*

The possible upconversion mechanism of the visible upconversion emission of Ho^{3+}-Yb^{3+} systems upon excitation at around 980 nm including energy transfer is shown in Fig. 4. The Yb^{3+} ion is excited from the ground state $^2F_{7/2}$ level to the excited state $^2F_{5/2}$ level, and then transfers its energy to a nearby Ho^{3+} ion populating the $^5I_6$ excited level. This is a phonon-assisted energy transfer process because of energy mismatch between the $^2F_{5/2}$ level of Yb^{3+} and $^5I_6$ level of Ho^{3+} [15]. The highest phonon energy of the $(WO_4)^{2-}$ group is about 900 cm^{-1} [16] and the energy separation between the $^2F_{5/2}$ and $^5I_6$ manifolds is about 1536 cm^{-1}, so the multiphonon relaxation from the $^2F_{5/2}$ level to the level $^5I_6$ is possible. The population in the $^5I_6$ level is promoted to $^5S_2$ level either by the absorption of a pump photon excited state absorption, or by energy transfer from another excited Yb^{3+} ion decaying to the ground state. It is supposed that the

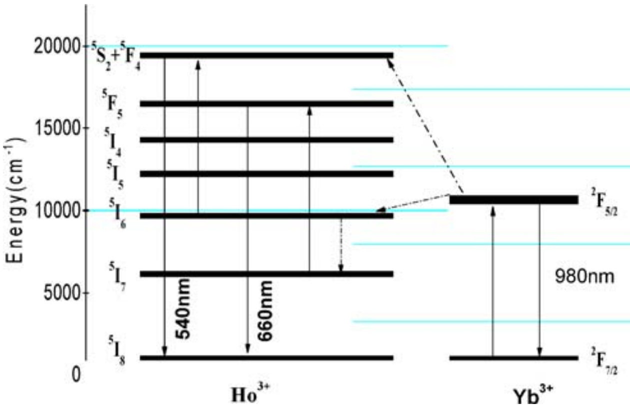

FIGURE 4 Scheme of energy levels for NGW:Ho^{3+}-Yb^{3+} upon excitation at around 980 nm. *Solid arrows* indicate transitions with absorption or emission of photons. *Dotted arrows* indicate nonradiative transitions

$^5F_5$ level is populated exclusively by excited state absorption from the $^5I_7$ level, which is fed by multiphonon relaxation from $^5I_6$. Finally, the $^5F_5$ or $^5S_2$ level is populated and part of the excited ions relax to the ground state producing the red or green emission.

3.3 *Assessment of laser potential associated with the upconverted red emission*

The most intense lines in the emission spectra shown in Fig. 2 correspond to transitions ending at the highest crystal-field components of the ground $^5I_8$ state [17]. This feature is extremely advantageous for potential laser operation since the $^5F_5 \to {}^5I_8$ transition considered corresponds to quasi-four-level operation in which the terminal level population is a critical factor [14].

The most important parameter influencing the potential laser performance of a material is the emission cross-section. The emission cross-section can be obtained by using the Füchtbauer–Ladengurg (F–L) formula [18]:

$$\sigma_{\mathrm{em}}(\lambda) = \frac{\lambda^5 \beta}{8\pi c n^2 \tau_{\mathrm{r}}} \frac{3 I_{\sigma,\pi}(\lambda)}{\int [2 I_{\sigma}(\lambda) + I_{\pi}(\lambda)] \lambda \, \mathrm{d}\lambda} \,. \tag{1}$$

Here $I_{\sigma,\pi}(\lambda)$ is the experimental emission intensity for σ or π polarization spectrum, c is the light velocity, n is the index of the refraction (here $n = 1.945$ [19]), β is the branching ratio, and τ_{r} is the radiative lifetime. The values of β and τ_{r} obtained from our previous publication [20] are 0.772 and 172 µs, respectively. The emission cross-sections were calculated for the $^5F_5 \to {}^5I_8$ transition and the shapes of $\sigma^{\sigma}_{\mathrm{em}}$ and $\sigma^{\pi}_{\mathrm{em}}$ curves derived are presented in Fig. 5. The maximum emission cross-section is $2.3 \times 10^{-20}\,\mathrm{cm}^2$ for π polarization spectrum at 660 nm and $2.0 \times 10^{-20}\,\mathrm{cm}^2$ for σ polarization spectrum at 659 nm. These values are comparable with those of $LiYF_4$:Ho^{3+} laser material ($2.6 \times 10^{-20}\,\mathrm{cm}^2$ for the π polarization spectrum at 657 nm and $2.2 \times 10^{-20}\,\mathrm{cm}^2$ for the σ polarization spectrum at 659 nm [18]). It should be noted that the calculated emission cross-sections should be treated as estimated values to be verified by laser experiments, because of the uncertainty of radiative transition rates and luminescence branching ratios, derived from a fitting procedure of the Judd–Ofelt theory. Efficiencies of absorption of IR light at 980 nm and of the Yb-Ho energy transfer in this system may be tailored by appropriate choice of donor and acceptor concentrations.

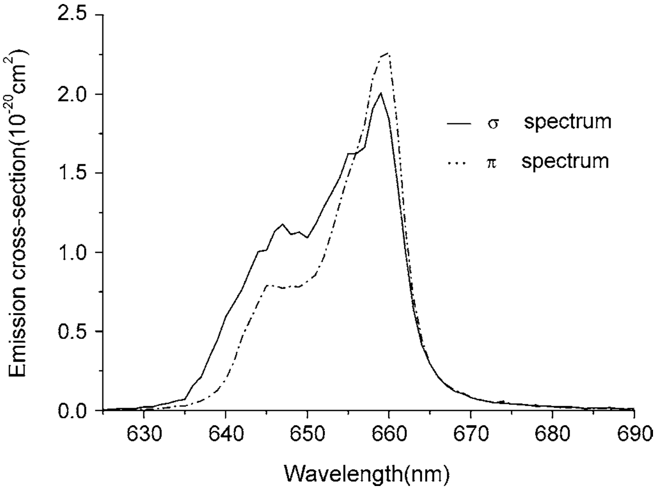

FIGURE 5 Emission cross-sections corresponding to $^5F_5 \to {}^5I_8$ transition of the NGW: 8 at. % Yb^{3+}, 4 at. % Ho^{3+} crystal

4 Conclusion

$NaGd(WO_4)_2$:Yb^{3+}, Ho^{3+} single crystals were grown successfully by the Czochralski technique. Conversion of the infrared (IR) radiation at 980 nm into the visible emission in $NaGd(WO_4)_2$ crystals containing several different concentrations of Yb^{3+} and Ho^{3+} has been investigated. The $NaGd(WO_4)_2$: 8 at. %Yb^{3+}, 4 at. % Ho^{3+} system exhibits intense red upconverted emission originating from the $^5F_5$ level with 980 nm excitation. The ratio of the red to green emission intensities is 10 : 1 at room temperature. The mechanism for the conversion of IR radiation into red emission centered at 660 nm in a $NaGd(WO_4)_2$:Yb^{3+}, Ho^{3+} system was reported. It is concluded that the green emission is excited by energy transfers from Yb^{3+} to Ho^{3+}, whereas excited state absorption is involved in the excitation of red emission. The emission cross-section of the $^5F_5 \to {}^5I_8$ transition in the $NaGd(WO_4)_2$: 8 at. %Yb^{3+}, 4 at. % Ho^{3+} crystal was estimated to be $2.3 \times 10^{-20}\,\mathrm{cm}^2$ for the π polarization spectrum at 660 nm and $2.0 \times 10^{-20}\,\mathrm{cm}^2$ for the σ polarization spectrum at 659 nm by using the Füchtbauer–Ladengurg formula. The upconversion described may be of interest in designing solid-state laser sources in the red. Results show that $NaGd(WO_4)_2$:Yb^{3+}, Ho^{3+} system may be a potential candidate for an upconverted red laser.

ACKNOWLEDGEMENTS This work was supported by the Innovative Project of Chinese Academy of Sciences (KJCX2-SW-h05), the Nature Science Foundation of Fujian Province of China (E0410028) and the Frontier & Interdisciplinary project of Fujian Institute of Research on the Structure of Matter, CAS.

REFERENCES

1 P. Müller, M. Wermuth, H.U. Güdel, Chem. Phys. Lett. **290**, 105 (1998)
2 A.J. Silversmith, W. Lenth, R.M. Macfarlane, J. Opt. Soc. Am. A **3**, 128 (1986)
3 L.F. Johnson, H.J. Guggenheim, Appl. Phys. Lett. **19**, 44 (1971)

4 B. Peng, T. Izumitani, Opt. Mater. **4**, 701 (1995)

5 T. Sandrock, H. Sheife, E. Heumann, G. Huber, Opt. Lett. **22**, 808 (1997)

6 D.S. Funk, S.B. Stevens, S.S. Wu, J.G. Eden, IEEE J. Quantum Electron. **QE-32**, 638 (1996)

7 M.V. Mokhosoev, V.I. Krivobok, S.M. Aleikina, Neorg. Mater. **3**, 1657 (1967)

8 J. Faure, N. Borel, C. Couchaud, Appl. Phys. B **63**, 593 (1996)

9 E.V. Zharikov, G.M. Kuz'micheva, D.A. Lis, Y.M. Papin, V.B. Rybakov, B.A. Smirnov, K.A. Subbotin, Inorg. Mater. **39**, 151 (2003)

10 Z. Cheng, Q. Lu, S. Zhang, J. Liu, X. Yi, F. Song, Y. Kong, J. Han, H. Chen, J. Cryst. Growth **222**, 797 (2001)

11 V. Volkov, C. Zaldo, J. Cryst. Growth **206**, 60 (1999)

12 H. Wang, G. Jia, F. Yang, Y. Wei, Z. You, Y. Wang, J. Li, Z. Zhu, X. Lu, C. Tu, Appl. Phys. B **83**, 579 (2006)

13 J.B. Gruber, M.E. Hills, M.D. Seltzer, S.B. Stevens, C.A. Morrison, G.A. Turner, M.R. Kokta, J. Appl. Phys. **69**, 8183 (1991)

14 W. Ryba-Romanowski, S. Golab, G. Dominiak-Dzik, P. Solarz, T. Lukasiewicz, Appl. Phys. Lett. **79**, 3026 (2001)

15 L. Feng, J. Wang, Q. Tang, L. Liang, H. Liang, Q. Su, J. Luminesc. **124**, 187 (2007)

16 A.A. Kaminskii, H.J. Eichier, K. Ueda, N.V. Klassen, B.S. Redkin, L.E. Li, J. Findeisen, D. Jaque, J. Garcia-Sole, J. Fernandez, R. Balda, Appl. Opt. **38**, 4533 (1999)

17 R. Lisiecki, G. Dominiak-Dzik, W. Ryba-Romanowski, T. £ukasiewicz, J. Appl. Phys. **96**, 6323 (2004)

18 B.M. Walsh, N.P. Barnes, B. Di Bartolo, J. Appl. Phys. **83**, 2772 (1998)

19 M. Rico, J. Liu, U. Griebner, V. Petrov, Opt. Express **12**, 5362 (2004)

20 H. Wang, J. Li, G. Jia, Z. You, F. Yang, Y. Wei, Y. Wang, Z. Zhu, X. Lu, C. Tu, J. Alloys Compd. **431**, 277 (2007)